

Performance Analysis of Full-Duplex DF Relay-Based D2D Communication with Energy Harvesting

Afina Nabila Dirganingsih, Anang Budikarso, Yoedy Moegiharto, Mohammad Ridwan, Faridatun Nadziroh, Budi Aswoyo

Politeknik Elektronika Negeri Surabaya, Jl Raya ITS Kampus PENS, Indonesia

**Corresponding author: Anang Budikarso email: anang_bk@pens.ac.id*

Manuscript received April 15, 2026, revised April 20, 2026, accepted April 21, 2026

Abstract – *Device-to-device (D2D) communication is a promising technology that leverages spectral efficiency and relieves network congestion in next-generation wireless systems. However, it suffers from significant performance degradation under Interference and limited transmission power and energy limitations, especially in the suburban areas with non-line-of-sight (NLOS) propagation conditions. To tackle these challenges, this paper studies a full-duplex D2D communication system with an energy-harvesting decode-and-forward (DF) relay based on the power-splitting relaying (PSR) protocol. The system model enables simultaneous information and energy transfer using radio-frequency (RF) signals as the energy source. We examine two scenarios: a relay-assisted self-interference model and a multi-node interference model. We evaluate system performance in terms of signal-to-noise ratio (SNR), throughput, and outage probability for different energy-harvesting efficiencies, power-splitting factors, and time-allocation parameters. Simulations show that system performance rises with energy-harvesting efficiency. We also identify optimal power-splitting and time-allocation values for maximum throughput. In the full-duplex DF relay system, self-interference is present at the relays, yet spectral efficiency improves. However, multiple nodes cancel each other out, causing a drop. These results help design effective, energy-efficient D2D communication systems with near-optimal performance for future wireless networks.*

Keywords: *D2D, Full Duplex, Energy Harvesting, Power Splitting Relaying, Decode and Forward Protocols*

I. Introduction

Device-to-device (D2D) communication has emerged as a key technology in next-generation wireless networks, enabling direct communication between nearby devices without relying on base stations [1]. However, despite its advantages, D2D communication faces several critical challenges that significantly affect system performance.

One of the main challenges is Interference, particularly in dense network environments where multiple D2D pairs share the same spectrum [2]. This issue becomes more severe in full-duplex systems, where simultaneous transmission and reception introduce self-interference and additional inter-node Interference. Another important limitation is energy availability, especially in suburban or non-line-of-sight (NLOS) environments, where transmission power is constrained, and energy efficiency becomes a critical factor.

Several studies have investigated D2D communication systems and relay-assisted transmission techniques. For example, prior work has explored decode-and-forward (DF) relaying and cooperative communication to improve link reliability [3]. However, many existing studies are limited to half-duplex systems, which suffer from reduced

spectral efficiency. Other works have considered energy harvesting techniques, but often without addressing the combined impact of interference and resource allocation [4]. Furthermore, the integration of full-duplex relaying with energy harvesting has not been sufficiently analyzed, particularly with respect to parameter optimization and system-level performance trade-offs.

To address these limitations, this paper proposes a full-duplex DF relay-based D2D communication system with energy harvesting using the power-splitting relaying (PSR) protocol. The proposed approach enables simultaneous information and energy transfer, allowing the relay to harvest energy from RF signals while forwarding data. This integration introduces a fundamental trade-off between energy harvesting and information transmission, which must be carefully analyzed to achieve optimal system performance [5].

While previous studies such as [4] and [5] have investigated full-duplex relaying and energy harvesting techniques, several important aspects remain insufficiently addressed. In [4], the analysis primarily focuses on half- and full-duplex relaying with energy harvesting but does not specifically consider their

integration within a D2D communication framework using power-splitting relaying (PSR). Similarly, [5] studies full-duplex relay systems with energy harvesting; however, the analysis is limited to general relay networks and does not explore parameter optimization in D2D scenarios. In contrast, this work introduces several key novelties. First, it integrates full-duplex decode-and-forward (DF) relaying with PSR-based energy harvesting specifically for D2D communication systems. Second, it considers two interference scenarios, namely relay self-interference and multi-node Interference, providing a more comprehensive performance evaluation. Third, this study performs a joint analysis of key system parameters, including energy harvesting efficiency (η), power splitting factor (β), and time allocation factor (α), and identifies their optimal values based on physical trade-offs. These aspects distinguish the proposed approach from existing works and provide deeper insights into the design of energy-efficient full-duplex D2D systems. Therefore, unlike [4] and [5], this work emphasizes the combined impact of energy harvesting, power allocation, and Interference in a full-duplex D2D system, which has not been thoroughly investigated in prior studies.

The main contributions of this paper are summarized as follows:

1. A full-duplex D2D communication system with an energy-harvesting DF relay based on the PSR protocol is developed.
2. Two system scenarios are analyzed: relay self-interference and multi-node Interference.
3. The impact of key parameters, including energy harvesting efficiency (η), power splitting factor (β), and time allocation factor (α), on system performance is investigated.
4. The optimal parameter values that maximize throughput and improve system reliability are identified through simulation.

II. System Model

Designing this model system is based on a cooperative communication D2D system. The design is applied to energy harvesting (EH) using the power-splitting relaying (PSR) protocol. Cooperative communication indirectly links the D2D system using the decode-and-forward protocol. The transmission uses a Relay (R) node between the Source (S) and Destination (D).

TABLE I

Notation	Description
S	Source node
R	Relay node
D	Destination node
d_{ij}	Distance from i to j
P_B	Transmission power from the Base Station
P_i	Transmission Power from the node
η_i	Energy Conversion Coefficient
β	Power splitting factor
α	Time splitting factor
h_{ij}	Coefficient Channel node i to node j
$ h_{ij} ^2$	Gain channel dari titik i ke j
m	Pathloss ekspone = 2.7
σ_{ij}^2	Variance of noise on each node
I_i	Residual loopback
γ_i	The received signal

The system model is depicted in Figures 1 and 2.

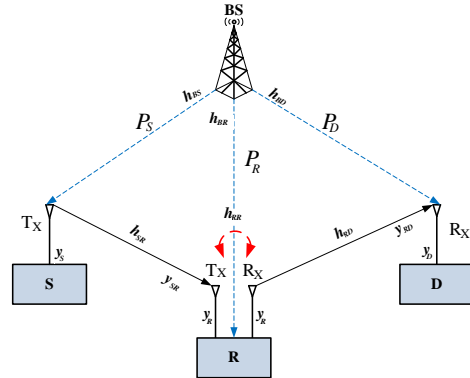


Fig. 1. Model System 1

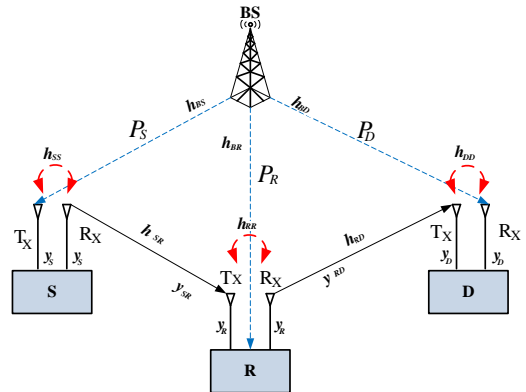


Fig. 2. Model System 2

This model system uses EH mode, harvesting Radio Frequency (RF) energy for each node S, R, and D via a coefficient channel that represents $h_{BS} = h_{BR} = h_{BD}$. Based on the EH result, the node-to-node transmission power (P) will be used. P comes from the utilization of channel gain from the absolute squared channel coefficients. In the DF protocol, node R decodes the data that arrives to remove noise; thus, it can be stated that the data from S has the same value as in node R. The model channel is Rayleigh, with the place assumption applied in suburban areas; therefore, the path loss is 2.7. On that matter, this model system has a Non-Line of Sight (NLOS) trait.

In the first model system (Fig. 1), the node antenna in R causes known self-interference, but in the second model (Fig. 2), self-interference occurs at every node. Although it has a different model, the Interference has the same type: loopback interference. There are three methods to break the signal code that have been expected. In this scenario, the interference Cancellation (SIC) method is modeled in Gaussian random variables, with the variance of σ_{SS}^2 , σ_{RR}^2 , dan σ_{DD}^2 . SIC produces residual, also known as I_S , I_R , and I_D .

This simulation will be measured with two calculations. Outage Probability (OP) will be used to measure transmission failure. The other Calculation is Throughput (τ) for measuring the success of transmitting data to the destination. The measurement uses the formulas of (1)- (2).

$$OP = P_R(\gamma_D < \gamma_{th}) \quad (1)$$

$$\tau = (1 - OP)R/2 \quad (2)$$

III. Performances System

1.1. Energy Harvesting Process

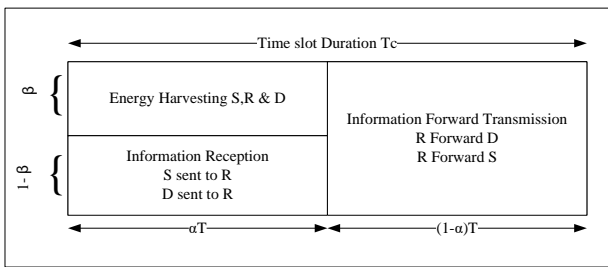


Fig. 3. Power Splitting Factor Performance

Before doing a transmission signal, TC will split into two sub-slots. In the first time slot, there will be two actions. First, energy harvesting is occurring at nodes S, R, and D, with β set to ($0 < \beta < 1$). Equations (3) – (5) provide the EH calculation on each node.

$$E_S = \beta \eta_s |h_{BS}|^2 d_{BS}^{-m} P_B \alpha T \quad (3)$$

$$E_R = \beta \eta_R |h_{BR}|^2 d_{BS}^{-m} P_B \alpha T \quad (4)$$

$$E_D = \beta \eta_D |h_{BD}|^2 d_{BS}^{-m} P_B \alpha T \quad (5)$$

From the EH Process, the transmission power can be obtained from the duration of the power-splitting factor β . The Calculation can be seen in formulation (6) – (8),

$$P_S = \frac{E_S}{\alpha T} = \beta \eta_s |h_{BS}|^2 d_{BS}^{-m} P_B \quad (6)$$

$$P_R = \frac{E_R}{(1-\alpha)T} = \beta \eta_R |h_{BR}|^2 d_{BS}^{-m} P_B \alpha T \quad (7)$$

$$P_D = \frac{E_D}{\alpha T} = \beta \eta_D |h_{BD}|^2 d_{BS}^{-m} P_B \quad (8)$$

1.2. Signal Transmission Process

A. Model System 1

In this applied scenario, node R will have self-interference h_{RR} . This technique would be called SIC. *Self-interference (SI) is considered a Gaussian random variable in this simulation.* SI will appear on transmission from S to R or during $1 - \beta$ on αT . When R receives the signal, there will be a distortion value from the S node. The decoding process in R is assumed to be equal to S. The signal that has been received can be calculated from equations (9) and (10).

$$y_R = (1 - \beta) \sqrt{P_S} \left(\frac{h_{SR}}{\sqrt{d_{SR}^m}} \right) x_S + (1 - \beta) \sqrt{P_D} \left(\frac{h_{RD}}{\sqrt{d_{RD}^m}} \right) x_D + \sqrt{P_R} h_{RR} x_R + \eta_R$$

$$= (1 - \beta) \left\{ \sqrt{P_S} \left(\frac{h_{SR}}{\sqrt{d_{SR}^m}} \right) x_S + \sqrt{P_D} \left(\frac{h_{RD}}{\sqrt{d_{RD}^m}} \right) x_D \right\} + \sqrt{P_R} h_{RR} x_R + \eta_R \quad (9)$$

$$y_D = (1 - \beta) \sqrt{P_R} \left(\frac{h_{RD}}{\sqrt{d_{RD}^m}} \right) x_S + n_D \quad (10)$$

When the signal arrives at the destination, the performance can be calculated using SNR through equations (11) and (12).

$$SNR_D = \frac{\text{Daya Informasi}}{\text{Noise}} = \gamma_R = \frac{(1 - \beta)^2 P_S H_{SR} + (1 - \beta)^2 P_D H_{RD}}{P_R H_{RR} + \sigma_R^2} \quad (11)$$

$$\frac{(1 - \beta)^2 ((\beta \eta_s |h_{BS}|^2 d_{BS}^{-m} P_B) H_{SR} + (\beta \eta_s |h_{BS}|^2 d_{BS}^{-m} P_B) H_{SR})}{(\beta \eta_R |h_{BR}|^2 d_{BS}^{-m} P_B) \sigma_{RR}^2 + \sigma_R^2}$$

$$\text{Where, } H_{SR} = |h_{SR}|^2 d_{BS}^{-m} \quad (12)$$

$$\gamma_D = \frac{P_R H_{RD}}{\sigma_D^2}$$

$$\gamma_D = \frac{(1-\beta)^2 P_R d_{RD}^{-m} |h_{RD}|^2}{\sigma_D^2} \quad (13)$$

Where $H_{RD} = |h_{RD}|^2 d_{BS}^{-m}$ is the AWGN model on throughput calculation with OP system fixed transmission, the measurement can be seen from equations (14),

$$\begin{aligned} \tau &= (1 - prob)R/2 \\ &= \frac{(1 - P_R(\gamma_D < \gamma_{th}))R}{2} \\ &= \frac{\left(1 - P_R\left(\frac{(1-\beta)^2 P_R d_{RD}^{-m} |h_{RD}|^2}{\sigma_D^2} < \gamma_{th}\right)\right)R}{2} \end{aligned} \quad (14)$$

Where R is the transmission rate,

B. Model System 2

The difference between the models is that in model system 2, there is an SIC function on each node. Another difference is that it will be assumed that S and D will receive the signal simultaneously, so that self-interference will appear in the transmission. At the destination, the information signal that emerges will be affected by signals from R and SIC, depending on the protocol used. Equations (15) and (16) are equal to the formulations as follows,

$$\begin{aligned} y_R &= (1 - \beta) \left\{ \sqrt{P_S} \left(\frac{h_{SR}}{\sqrt{d_{SR}^m}} \right) x_S \right. \\ &\quad \left. + \sqrt{P_D} \left(\frac{h_{RD}}{\sqrt{d_{RD}^m}} \right) x_D \right\} \\ &+ \sqrt{P_R} h_{RR} x_R + \eta_R \end{aligned} \quad (15)$$

$$\begin{aligned} y_D &= y_D = (1 - \beta) \sqrt{P_R} \left(\frac{h_{RD}}{\sqrt{d_{RD}^m}} \right) x_R + \\ &(1 - \beta) \sqrt{P_D} h_{DD} x_D + \eta_D \end{aligned} \quad (16)$$

Where n_r AWGN is represented by σ_R^2 and σ_D^2 [17][18] as influenced by SIC that will produce residual loopback interference channels, whereas residual $h_{RR}x_R$ and $h_{DD}x_D$ will be changed to SIC I_R dan I_D as a substitute, equations (17)-(18) can be written as,

$$\begin{aligned} y_R &= (1 - \beta) \left\{ \sqrt{P_S} \left(\frac{h_{SR}}{\sqrt{d_{SR}^m}} \right) x_S \right. \\ &\quad \left. + \sqrt{P_D} \left(\frac{h_{RD}}{\sqrt{d_{RD}^m}} \right) x_D \right\} + \\ &\sqrt{P_R} I_R + \eta_R \end{aligned} \quad (17)$$

$$\begin{aligned} y_D &= (1 - \beta) \sqrt{P_R} \left(\frac{h_{RD}}{\sqrt{d_{RD}^m}} \right) x_R + \\ &(1 - \beta) \sqrt{P_D} I_D + \eta_D \end{aligned} \quad (18)$$

With equations (19) as formulations of the SNR signal,

$$\begin{aligned} \tau &= (1 - prob)R/2 \\ &= \frac{(1 - P_R(\gamma_D < \gamma_{th}))R}{2} \\ &= \frac{\left(1 - P_R\left(\frac{(1-\beta)^2 P_R d_{RD}^{-m} |h_{RD}|^2}{(1-\beta)^2 P_D \sigma_{DD}^2 + \sigma_D^2} < \gamma_{th}\right)\right)R}{2} \end{aligned} \quad (19)$$

IV. Results and Discussion

The simulation will be done with parameter variances changing, but some parameters will not be changed. That parameter would be attached to Table II.

TABLE II

Parameter	Measurements
Binary Input	10 ⁵
Channel Model D2D Link	Rayleigh Channel Fading
Relaying Protocol	Decode and Forward
Path Loss Exponent between D2D Link	2.7
Efficiency Factor S Energy Harvesting	0.5
Efficiency Factor D Energy Harvesting	0.5
Efficiency factor R	Max 0.8
Energy Harvesting	0.5
Power Splitting Factor	Max 0.8
Time Splitting Factor	Max 0.8
Transmission Rate	2
Base Station Power	20 dB; 26 dB
Distance S to R	Max 15 meters
Distance S to D	20 meter
Distance D to R	Max 15 meters
Distance BS to S	100 meter
Distance BS to R	100 meter
Distance BS to D	100 meter

The evaluation is designed to determine the system's optimal performance by observing how the parameter changes over time. The optimal design will be shown from throughput and outage probability measurements. The parameter evaluation that will be changed consists of :

1. Variance of the EH efficiency value on the relay or η_R
The efficiency factor affects the EH process at each node. A change in the efficiency factor parameter at node R (η_R) will affect the energy obtained from the base station to the relay. Based on this statement, it also affects the SNR at the end node.
2. Variance of the power splitting factor or β
The system is divided into two sub-slots within one transmission duration. In the first sub-slot, two events occur: the EH process and the transmission process of information signals. In this sub-slot, power allocation is performed by adjusting the β coefficient. The value of β ranges between ($0 < \beta < 1$).
3. Variance of the time splitting factor or α
The time allocation factor, also referred to as α , is influential due to the time slot allocation, as shown in Figure 3. This time allocation indicates when the EH time and the transmission of S, D to R or R to S, D occur. The coefficient α ranges between ($0 < \alpha < 1$).

A. Model System 1

- Variance value of the parameter η_R

This testing is conducted by varying the parameter η_R or the EH efficiency factor at the relay. The efficiency changes at the relay use values ranging from 0.1 to 0.8 for EH. The test results are attached in Fig. 4.

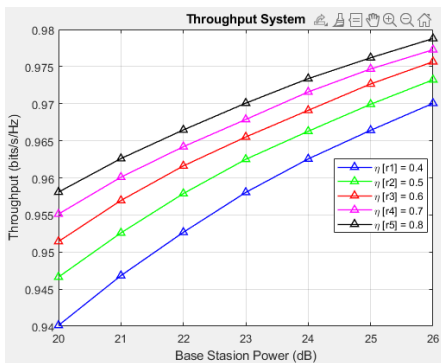


Fig. 4. Throughput η_R First Model System

Figure 4 is based on variations in the EH efficiency factor η_R at node R, ranging from 0.1 to 0.8 for η_R . The observations made are $P_{BS} = 26 \text{ dBW}$ dBW and $\beta = 0.5$. The highest throughput is obtained at $\eta_R = 0.8$.

TABLE III
Evaluation Performance Throughput η_R .

$P_{BS} = 26 \text{ dBW}$				
η_R	P_R (mW)	SNR ($\times 10^3$)	SNR (dBW)	τ
0,1	0,51	8,21	39,14	0,9400
0,2	1	16,41	42,15	0,9580
0,3	1,5	24,62	43,91	0,9655
0,4	38	115,91	50,94	0,9700
0,5	48	144,88	51,61	0,9732
0,6	58	173,86	52,40	0,9757
0,7	67	202,83	53,07	0,9773
0,8	77	231,81	53,65	0,9788

Figure 4 stems from variations in the EH efficiency factor η_R at node R, with values ranging from 0.1 to 0.8 for η_R . The observations made are $P_{BS} = 26 \text{ dBW}$ and $\beta = 0.5$. The highest throughput is achieved at $\eta_R = 0.8$, with a value of 0.9788 bps/Hz. The results show that the SNR increases with η_R , implying that data transmission success is higher when the EH efficiency is higher. From the throughput value in Table III, it is evident that the transmitted data succeed upon reaching D. This result can be compared with the outage probability, leading to the conclusion that failures will be fewer when the SNR is high, which is significantly influenced by the enhanced EH process outcomes at node R.

Figure 4 illustrates the effect of the energy harvesting efficiency at the relay (η_R) on system throughput. The throughput increases with η_R , reaching a maximum at $\eta_R = 0.8$. This behavior can be explained by the fundamental role of energy harvesting efficiency in determining the available transmit power at the relay. Specifically, the harvested energy is proportional to the efficiency factor η , which directly influences the relay's ability to forward the received signal. As η increases, more RF energy is converted into usable electrical energy, thereby increasing transmit power. Consequently, the signal-to-noise ratio (SNR) at the destination improves, leading to increased throughput and reduced outage probability. Conversely, when η is low, the limited harvested energy restricts the relay transmission capability, resulting in degraded SNR and poorer system performance. Therefore, the observed performance improvement is not merely a simulation result but reflects the fundamental relationship between energy harvesting efficiency and system reliability in wireless communication systems.

This trend can be explained by the direct relationship between energy harvesting efficiency and the available transmit power at the relay. A higher η_R allows the relay to convert more RF energy into usable electrical energy, thereby increasing its transmission capability. As a result, the signal-to-noise ratio (SNR) at the destination improves, increasing the probability of successful data transmission.

Conversely, when η_R is low, the harvested energy is insufficient to sustain reliable forwarding, leading to lower SNR and degraded system performance. Therefore,

improving energy-harvesting efficiency is crucial to enhancing throughput performance.

- Variance value of parameter β

This observation relies on the value of parameter β for optimization. Based on this observation, the throughput and SNR values are expected to be observed at node D. The results are displayed in Figure 5.

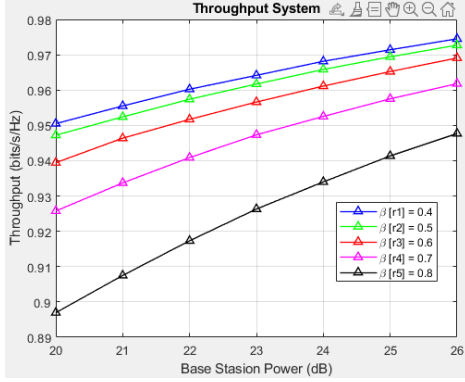


Fig. 5. Throughput β First Model System

Figure 5 shows that $\beta=0.4$ yields the highest success rate, with $\eta=0.4$. The data parameter achievements are displayed in Table IV.

TABLE IV
EVALUATION PERFORMANCE THROUGHPUT β

$P_{BS} = 26 \text{ dBW}$				
β	P_R (mW)	SNR ($\times 10^3$)	SNR (dBW)	τ
0,1	0,24	5,963	37,76	0,9655
0,2	0,48	9,424	39,74	0,9722
0,3	0,73	10,823	40,34	0,9743
0,4	1,1	13,902	41,43	0,9746
0,5	1,4	12,068	40,82	0,9728
0,6	1,7	9,268	39,67	0,9689
0,7	1,9	6,082	37,84	0,9617
0,8	2,2	3,089	34,89	0,9464

Figure 5 shows that the system achieves its optimal throughput at $\beta \approx 0.4$. While the descriptive results indicate a peak at this value, the underlying reason is governed by a fundamental trade-off in the power-splitting relaying (PSR) protocol.

Specifically, β determines how the received signal power is divided between energy harvesting and information processing. When β is too small, only a limited portion of the signal is used for energy harvesting, resulting in insufficient energy to support reliable transmission at the relay. Consequently, the transmit power decreases, leading to lower SNR and reduced throughput.

On the other hand, when β is too large, a significant portion of the signal power is allocated for energy harvesting, leaving insufficient power for information decoding and transmission. This degrades signal quality and reduces system performance.

Therefore, an intermediate value of β provides an optimal balance between energy harvesting and information transmission. In this study, $\beta \approx 0.4$ yields the best performance, maximizing throughput.

- Variance value of parameter α

This section examines the performance impact of varying the α parameter on throughput.

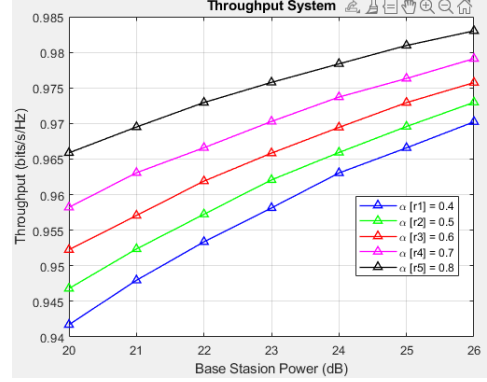


Fig. 6. Throughput α First Model System

TABLE V
EVALUATION PERFORMANCE THROUGHPUT α

$P_{BS} = 26 \text{ dBW}$				
α	P_R (mW)	SNR ($\times 10^4$)	SNR (dBW)	τ
0,1	1,4	2,098	43,22	0,9634
0,2	1,5	2,361	43,73	0,9657
0,3	1,7	2,698	44,31	0,9679
0,4	2,5	4,846	46,85	0,9702
0,5	3,0	5,816	47,65	0,9730
0,6	3,8	7,269	48,66	0,9757
0,7	5,1	9,693	49,86	0,9791
0,8	7,6	14,539	51,63	0,9830

In addition to the test graph in Figure 6, Figure 6 presents the relationship between the time allocation factor α and system throughput. It is observed that throughput increases with increasing α . This behavior reflects a trade-off between the duration of energy harvesting and the time required for data transmission. Increasing α allows more time for energy harvesting, enabling the relay to accumulate more energy and thereby enhancing transmission power and improving SNR. However, allocating too much time to energy harvesting reduces the duration available for data transmission. This may limit the effective data rate if the transmission phase becomes too short. Therefore, although increasing α improves energy availability, an appropriate balance is required to optimize overall system performance.

Table V shows that as α increases, throughput increases. However, even as the SNR rises, it can be estimated that as the time lengthens, the speed also increases, meaning more time is spent sending data to R than sending data from R to the destination.

B. Model System 2

- Variance value of the parameter η_R

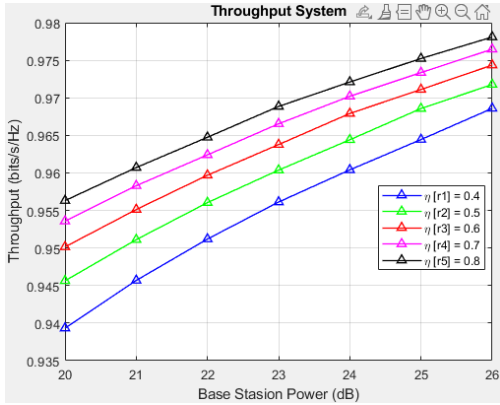


Fig. 7. Throughput η_R Second Model System

Figure 8 is based on variations in the EH efficiency factor η_R at node R, ranging from 0.1 to 0.8 for η_R . The observations made are $P_{BS} = 26$ dBW and $\beta = 0.5$. The highest throughput is achieved at $\eta_R = 0.8$. Similar to Model System 1, throughput increases with η_R , reaching its maximum at $\eta_R = 0.8$. However, the overall performance is slightly lower than that of Model System 1. This is due to additional self-interference across multiple nodes. The Interference reduces the effective SNR at the receiver, limiting the performance gain obtained from increased harvested energy. This result highlights that while energy harvesting improves transmission capability, interference mitigation remains essential in full-duplex systems.

TABLE VI
EVALUATION PERFORMANCE THROUGHPUT η_R

$P_{BS} = 26$ dBW				
η_R	P_R (mW)	SNR ($\times 10^3$)	SNR (dBW)	τ
0,1	0,41	1,49	31,74	0,9379
0,2	0,83	2,98	34,75	0,9556
0,3	1,2	4,48	36,51	0,9634
0,4	1,6	5,97	37,76	0,9686
0,5	2,1	7,46	38,73	0,9718
0,6	2,5	8,95	39,52	0,9744
0,7	2,9	10,44	40,19	0,9765
0,8	3,3	11,93	40,77	0,9781

The highest result is obtained from the observed throughput at the most significant EH value of 0.8. This result yields a throughput value lower than the model's, at 0.9781 bps/Hz.

- Variance value of parameter β

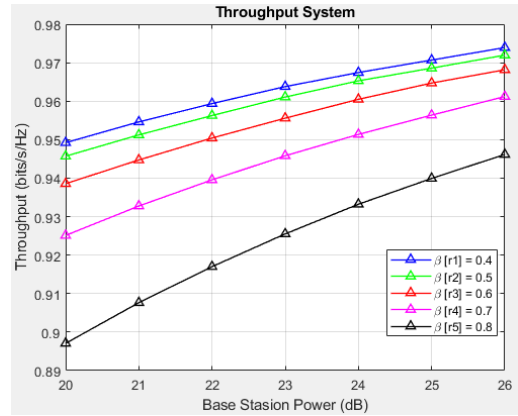


Fig. 8. Throughput β Second Model System

As shown in Fig. 8, the optimal value of β remains around 0.4, consistent with Model System 1. This confirms that the trade-off between energy harvesting and information transmission is a fundamental characteristic of PSR-based systems. However, the achieved throughput is slightly lower due to the increased Interference in Model System 2. Even with optimal power allocation, Interference degrades signal quality and limits performance.

TABLE VII
EVALUATION PERFORMANCE THROUGHPUT β

$P_{BS} = 26$ dBW				
β	P_R (mW)	SNR ($\times 10^3$)	SNR (dBW)	τ
0,1	0,25	3,19	35,05	0,9659
0,2	0,51	3,91	35,92	0,9725
0,3	0,75	4,12	36,14	0,9743
0,4	1,0	4,09	36,12	0,9739
0,5	1,3	3,89	35,89	0,9720
0,6	1,5	3,48	35,41	0,9682
0,7	1,8	2,82	34,49	0,9612
0,8	2,0	1,83	32,61	0,9462

In Table VII, the highest throughput is observed at $\beta = 0.4$. This indicates that as the β value increases, the throughput value decreases. The highest achieved result is 0.9739 bps/Hz.

- Variance value of parameter α

This simulation's test results show impacts approximately similar to those of the first model regarding the variance of α .

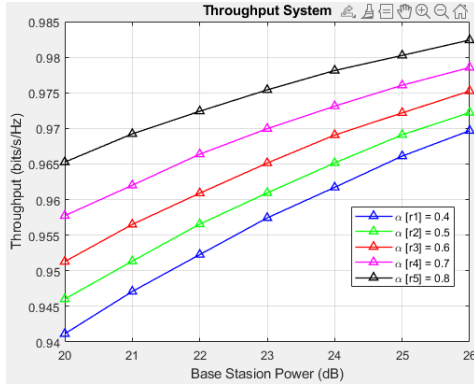


Fig. 9. Throughput α Second Model System

Figure 9 shows that throughput increases with α , following a similar trend as in Model System 1. Increasing α provides more time for energy harvesting, which improves transmission power and SNR. Nevertheless, due to additional Interference, the performance improvement is slightly constrained. This indicates that optimal system performance depends not only on time allocation but also on effective interference management.

TABLE VIII
EVALUATION PERFORMANCE THROUGHPUT α

$P_{BS} = 26 \text{ dBW}$				
α	P_R (mW)	SNR ($\times 10^3$)	SNR (dBW)	τ
0,1	0,75	2,34	33,69	0,9622
0,2	0,84	2,63	34,21	0,9643
0,3	0,96	3,01	34,79	0,9667
0,4	1,0	3,12	34,93	0,9697
0,5	1,2	3,73	35,72	0,9722
0,6	1,5	4,67	36,69	0,9752
0,7	2,0	6,22	37,94	0,9786
0,8	3,1	9,33	39,70	0,9824

Table VIII shows that throughput increases with α under the same conditions, with the SNR rising as other parameters increase. However, compared to the first model, the optimal value is found there.

V. Conclusion

From the results and discussion, the following conclusions are obtained.

- When changing the EH efficiency factor parameter at node R (η_R), the SNR and throughput increase with η_R , and the transmission power's download capacity also increases.
- The performance results of changing the power splitting parameter (β) indicate that the obtained SNR decreases as the value of β increases. For power allocation in the first sub-slot, if β is large, the energy received during EH will be greater, but for the second sub-slot, it implies that the EH value obtained is insufficient.

- The smaller the α value, the larger the throughput. The SNR value increases because, as the duration lengthens, the time for S to send data to R is longer than the time for R to send data to the destination. However, this figure should also be considered because if α is too large, the delivery time to D will be reduced.
- Comparing the two models, the second has a higher failure rate than the first. Nevertheless, its performance is satisfactory for delivery.
- From the two models, the highest value obtained after parameter changes in the first model, with $\eta_R=0.5$ and $\beta=0.5$ at the interference node R, $\alpha=0.8$, and $P_{BS} = 26 \text{ dBW}$, is 414.539×10^4 . The throughput performance results are $\tau = 0.9830 \text{ bps/Hz}$ and $P_{out} = 0.0170$.

References

- D. P. Hadyanto, D. S. Novariana, and A. Wulandari, "Device-to-Device in 5G," *Advances in Engineering Research*, pp. 649-654, 2021.
- T. L. Nguyen and Y. Shin, "Performance Analysis for Energy Harvesting Based Wireless Relay Systems," *2019 Asia Pacific Wireless Communication Symposium (APWCS)*, 2019.
- M. M. Salim, D. Wang, Y. Liu, H. A. E. A. Elsayed, and M. A. Elaziz, "Optimal Resource and Power Allocation With Relay Selection for RF/RE Energy Harvesting Relay-Aided D2D Communication," *IEEE ACCESS*, vol. 7, pp. 89670-89686, 2019.
- H. Sun, F. Han, S. Zhao, and H. Deng, "Half-Duplex and Full-Duplex DF Wireless Energy Harvesting Relaying in Rayleigh Fading," *Energies*, vol. 15, 2022.
- B. C. Nguyen, X. H. Le, V. D. Nguyen, and L. T. Dung, "On the Capacity of Full-Duplex AF/DF Relay System with Energy Harvesting for Vehicle-to-Vehicle Communication," *Hindawi*, vol. 2021, p. 11, 2021.
- A. T. A. N. T. Malik and A. J. A. Yasiri, "Relaying protocols for wireless energy harvesting and information processing," *Int. J. Eng. Adv. Technol.*, vol. 9, no. 1, pp. 1740-1746, 2019.
- S. A. K. S. P. and P. C., "Symbol Error Rate Performance of Hybrid DF/AF Relaying Protocol Using Particle Swarm Optimization Based Power Allocation," *International Conference on Advances in Computing and Communication Engineering (ICACCE)*, pp. 1-5, 2019.
- Y. Ye, Y. Li, L. Shi, R. Q. Hu, and H. Zhang, "Improved Hybrid Relaying Protocol for DF Relaying in the Presence of a Direct Link," *IEEE Wireless Communications Letters*, vol. 8, pp. 173-176, 2019.
- Arifin, A. Aprilya, M. C. Mayarakaca, F. Nadziroh, and Y. Moegiharto, "The UAV Assisted Wireless Powered on D2D Communication Hybrid AF/DF Multi Relay Based," *2023 International Electronics Symposium (IES)*, Vols. 192-198, 2023.
- H. Ghavami and B. Akhbari, "Secure resource allocation in device-to-device communications underlying cellular networks," *China Communications*, vol. 19, pp. 149-167, 2022.
- S. Ghosh, T. Acharya, and S. P. Maity, "Outage Analysis in SWIPT Enabled Cooperative AF/DF Relay Assisted Two-Way Spectrum Sharing Communication," *IEEE Transactions on Cognitive Communications and Networking*, vol. 8, pp. 1434-1443, 2022.
- S. Samy, E. Maher, and A. El-Mahdy, "Full-Duplex Relay-Aided D2D Communication in Heterogeneous Network with Imperfect CSI," *2020 16th International Computer Engineering Conference (ICENCO)*, pp. 181-186, 2020.
- H. Wu, Y. Zou, W. Cao, Z. Chen, T. Tsiftsis, M. R. Bhatnagar, and R. C. De Lamare, "Impact of Hardware Impairments on Outage Performance of Hybrid Satellite-Terrestrial Relay Systems," *IEEE Access*, vol. 7, pp. 35103-35112, 2019.

- [14] J. Lee and J. H. Lee, "Performance Analysis and Resource Allocation for Cooperative D2D Communication in Cellular Networks With Multiple D2D Pairs," *IEEE Communications Letters*, vol. 23, pp. 909-912, 2019.
- [15] Y. Zhang, W. Wang, X. Zhao, and J. Hou, "Performance analysis in SWIPT-based bidirectional D2D communications in cellular networks," *China Communications*, vol. 20, no. 12, pp. 41-51, 2023.
- [16] M. A. Bellido-Manganell and M. Walter, "Non-Stationary 3D M2M Channel Modeling and Verification with Aircraft-to-Aircraft, Drone-to-Drone, Vehicle-to-Vehicle, and Ship-to-Ship Measurements," *IEEE Transactions on Vehicular Technology*, pp. 1-16, 2023.
- [17] J. Jose, A. Agarwal, P. Shaik, V. Goyal, K. Choi, and V. Bhatia, "Performance Analysis and Learning-Assisted Power Control for NOMA Enabled D2D-Cellular Network," *IEEE Systems Journal*, pp. 1-4, 2023.
- [18] S. Akiishi, A. Ali, and E. Esenogho, "Interference Challenges on 5G Networks: A Review," *2023 IEEE AFRICON*, pp. 1-6, 2023.
- [19] S. Feng, X. Lu, D. Niyato, E. Hossain, and S. Sun, "Achieving Covert Communication in Large-Scale SWIPT-Enabled D2D Networks," *IEEE Transactions on Wireless Communications*, pp. 1-1, 2023.
- [20] M. Sadehvand, N. Moghim, B. S. Ghahfarokhi, and S. Shetty, "Transmission Power Control for Interference Reduction in Cellular D2D Networks," *2023 International Symposium on Networks, Computers and Communications (ISNCC)*, pp. 1-6, 2023.
- [21] H. Sun, R. Q. Hu, and Y. Qian, "5G Wireless Networks with Underlaid D2D Communications," *5G and Beyond Wireless Communication Networks*, pp. 10-20, 2024.
- [22] Z. Chen, J.-Y. Deng and H. Liu, "Dielectric Resonator Antenna Array," *Dielectric Resonator Antennas: Materials, Designs and Applications*, pp. 90-123, 2024.
- [23] M. M. Matalgah and M. A. Alqodah, "UAV Wireless Networks and Recorders," *Real-Time Ground-Based Flight Data and Cockpit Voice Recorder: Implementation Scenarios and Feasibility Analysis*, pp. 127-134, 2024.
- [24] T. A. Nugraha, "Relay Selection and Power Control in D2D-enabled Vehicular Communication," *2023 3rd International Conference on Electronic and Electrical Engineering and Intelligent System (ICE3IS)*, pp. 186-189, 2023.
- [25] M. Sadehvand, N. Moghim, B. S. Ghahfarokhi, and S. Shetty, "Transmission Power Control for Interference Reduction in Cellular D2D Networks," *2023 International Symposium on Networks, Computers and Communications (ISNCC)*, pp. 1-6, 2023.